

Design of the virtual model of re-drawing process

C. Maier¹, Kosmalski N.², M. Banu¹,
Epureanu Al.¹, Paunoiu V.¹

¹Universitatea "Dunărea de jos" Galați, Facultatea de Mecanică

²Ecole des Mines de Douai, France

ABSTRACT

This paper deals with the develop the finite element modelization of the re-drawing process in order to create his virtual model. The finite element is a method that permits to reduce the time and the cost in the designing. Then in a second time a good finite element model permit to avoid or complement laboratory characterization of material for re drawing. methodology for developing a laboratory inverse re-drawing device. The drawing process is performed in two phases: a direct drawing of a circular blank followed by a second reverse re-drawing phase on the same device.

A work is also done on the finite element model for the single deep drawing. This single deep drawing is used to validate the parameters of the numerical model. The main goal of this simulation is to define geometrical parameters of the process, in order to design a reverse re-drawing machine, and have the possibility in the future to compare experimental results and finite element results. The second goal is the estimation of the blank reaction (ability to support the process), and eliminate as well the default obtain during the simulation.

Keywords: finite element simulations, inverse re-drawing, strain path

1. Introduction

This study deals with the creation of a finite elements simulation of a reverse deep redrawing process. The re drawing is a process decomposed in several stages, and permit to obtain better results than a single step drawing (part 2).

Firstly, the goal is to determined correct numerical parameters (part 3.3) for a simulation of deep drawing. This research is based upon the comparison between a single drawing experimentation (part 3.1) and the result of the simulation of this experience (part 3.2).

The parameters is used in the simulation of the reverse drawing (part 4) in order to dimension reverse deep drawing tools parameters (clearance between the punch and the die/round radius of the punch and the die). A good simulation also permits to avoid or complement laboratory characterization of reverse deep drawing process.

2. Generality on reverse drawing

The severity of a deep drawing pass on a metal blank could be represented by the draw ratio

that is defined as $\beta = D_o/d_o$ (where D_o is the blank diameter and d_o the punch diameter). A blank with a certain thickness and material characteristics, has a draw ratio limit β_{lim} which represent the most severe operation that it can be submit to. In this way a blank could pass through a deep drawing operation if $\beta < \beta_{lim}$.

When high drawing ratios is required the process is decomposed into several steps. There are usually two kinds of redrawing: the direct and the reverse one.

The direct re-drawing use punch travel in the same time whereas reverse re-drawing punch travel in the opposite direction. Logically, the thickness reduces due to the first pass makes that the limiting draw ratio has to be decrease for the next steps:

$$\frac{d_o}{e} = k \cdot \beta_{lim} \quad (1)$$

where:

e - steel thickness

k - proportionality factor.

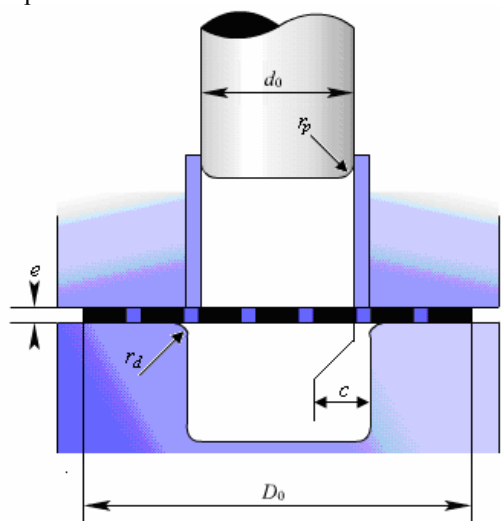
In the facts, we observe that β_{2lim} (limit drawing ratio on the second step) is superior to the estimation of β_{2lim} based on the thickness

reduction. The modification of the hardening parameters due to the first pass and the bending-unbending effects when sheet pass in the second step enhanced the material drawing properties.

3. Validation of a finite element model

The comparison between the model and the experiments is realized for the HSLA steel (cf. tab 1). The FEM also was realized for the DP600 steel. Both of them steels are designed for drawing operation.

Is detailed below, the geometrical parameters both used in the model and in the experimentation



Punch diameter	$d_o = 82.36\text{mm}$
Punch round radius	$r_p = 5.5\text{mm}$
Blank thickness	$e = 1\text{mm}$
Blank diameter	$D_o = 138\text{mm}$
Die round radius	$r_d = 8\text{mm}$
Clearance	$c = 1.3\text{mm}$
Drawing depth	$P = 41\text{mm}$

Fig. 1 - Geometrical parameters.

The draw ratio (i.e. severity of the pass defined as $\beta = D_o/d_o$ - cap.1) of the operation is $\beta=1.67$. The limiting draw ratio (the severity that steel can be submit to) for HSLA steel in our case is $\beta_{lim}=1.81$.

Tab 1 - Material properties

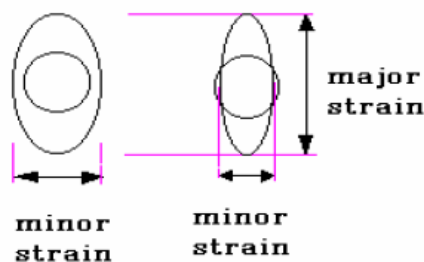
Material	Y_0 [Mpa]	R_m [Mpa]	E [Mpa]	ν
DP600	260	840	210000	0.33
HSLA	370	530	210000	0.33

Tab 2 - Power law parameters

Material	A	m	E [Mpa]	ν
DP600	1093	0.187	210000	0.33
HSLA	673	0.131	210000	0.33

3.1 The experimental procedure

A 3 mm diameter circle (dini) patterns is printed on the blank. When the drawing is done, the circle's deformation were measured by electronic microscope and given the major and minor strain



tension-tension tension-compression

Fig. 2 - Deformation of the grid

Tab 3 - Circle's deformation

i	d maj.	d min.	
1	4,649	1,806	Wall of cup
2	4,871	1,884	
3	4,21	1,993	
4	4,24	2,053	
5	4,16	2,446	
6	3,245	2,621	
7	3,146	3,043	Bottom of cup
8	3,006	3,046	
9	3,052	3,234	
10	3,154	3,217	
11	3,154	3,117	
12	3,142	3,032	

The circle 12 is tangent at the center, and circles indexes from 12 to 7 are disposed on the base of the cup. The circle 1 is on the blank border and circles 1 to 6 are disposed, from the border, n the wall of the drawn cup. The circle on the cup round can't be measured.

From these measures, the major and the minor strain (ϵ_1, ϵ_2) are calculated:

$$\epsilon_1 = \ln(d_{maj}/d_{ini}) ; \epsilon_2 = \ln(d_{min}/d_{ini}) \quad (2)$$

Then the thickness strain (ϵ_3) is deduced with the volume conservation rule:

$$\epsilon_1 + \epsilon_2 + \epsilon_3 = 0 \quad (3)$$

Assumed that is a plane stress model, (normal forces on contact are neglected) the stress is calculated with Lévy-Von Mises criteria:

Hook rules:

$$\begin{cases} \epsilon_x = \frac{1}{E} [\sigma_x - \mu(\sigma_y + \sigma_z)] \\ \epsilon_y = \dots \\ \epsilon_z = \dots \end{cases} \quad \zeta_{xy} = G \cdot \sigma_{xy} \quad (4)$$

So it can be deduced the stress :

$$\begin{cases} \sigma_x = 2G \left[\epsilon_x + \frac{\mu}{1-2\mu} (\epsilon_x + \epsilon_y + \epsilon_z) \right] \\ \sigma_y = \dots \\ \sigma_z = \dots \end{cases} \quad (5)$$

This relation is obtained :

$$\frac{\sigma_x - \sigma_y}{\epsilon_x - \epsilon_y} = \frac{\sigma_y - \sigma_z}{\epsilon_y - \epsilon_z} = \frac{\sigma_z - \sigma_x}{\epsilon_z - \epsilon_x} = 2G \quad (6)$$

In general case :

$$\frac{\sigma_1 - \sigma_2}{\epsilon_1 - \epsilon_2} = \frac{\sigma_2 - \sigma_3}{\epsilon_2 - \epsilon_3} = \frac{\sigma_3 - \sigma_1}{\epsilon_3 - \epsilon_1} = cste \quad (7)$$

In the situation of plane stress:

$$\frac{\sigma_1 - \sigma_2}{\epsilon_1 - \epsilon_2} = \frac{\sigma_2}{\epsilon_2 - \epsilon_3} \quad (8)$$

Huber-Mises-Hencky plastic criteria:

$$\sigma_{max} - \sigma_{min} = \beta \sigma_0 \quad \text{with } \beta = 1.1 \quad (9)$$

In our case if $\sigma_1 > \sigma_2$ then $\sigma_1 - \sigma_2 = \beta \sigma_0$

So the stress can be deduce from strain :

$$\frac{\epsilon_3 - \epsilon_1}{\epsilon_2 - \epsilon_1} \cdot \beta \cdot \sigma_0 = \sigma_1; \quad \frac{\epsilon_2 - \epsilon_3}{\epsilon_1 - \epsilon_2} \cdot \beta \cdot \sigma_0 = \sigma_2 \quad (10)$$

3.2 The numerical model

The finite element simulation is realized with the implicit code MscMarc. A two dimensions model is used with linear quad elements and with the large strain multiplicative option and use coulomb friction. The material is defined as elasto-plastic and use a power law modelisation (Swift law) :

$$\sigma = A \epsilon^m \quad (11)$$

Tab 4 - Parameters of the simulation

The optimize parameters	
Relative sliding velocity	0.075
Friction coefficient	0.01
Contact	0.01
Contact bias	0.1

3.3 Comparison between simulation and experimentation

Here a good strain correlation between the result of the FEM and experimentation is observed: 0,88 for the major strain and 0,97 for the minor strain.

The axy-symmetric simulation gives results close to the experimentation but there is anyway a gap between the series of strain. The average difference in the wall strain is about 20% and more than 100% in the bottom of the cup. Anyway, the simulation gives usable and coherent in the wall. And underestimation of 20% of the maximum strain value in the wall has to be taken in account to obtain coherent results. But the results in the bottom of cup are unusable.

The plane stress simulation doesn't give good strain results because the compressive stress under the blank holder is not applied on elements. And so only the stress due to the die round radius is involved in the model, what it explain the tray allure for the strain in the wall (see the plane stress modelization strain in the figure 3 and 4).

Contrary to the plane stress model, axy-symmetric model take in account the compressive stress and so gives better results.

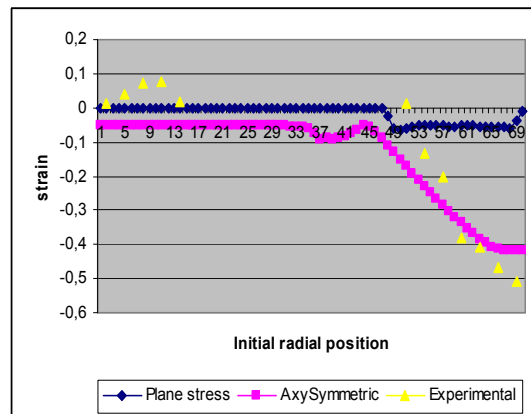


Fig 3- Minor strain for the two FEM modelization and experimental datas.

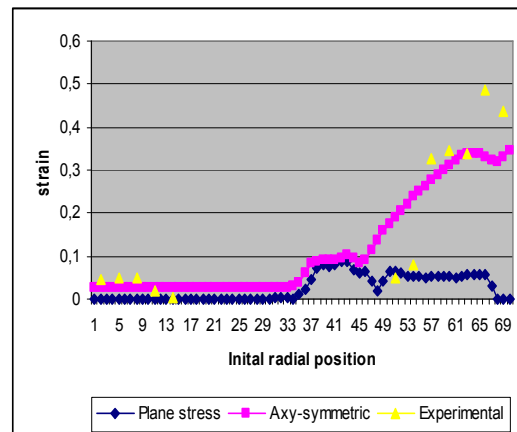


Fig 4 - Major strain

4. Reverse re-drawing simulation

In order to create a laboratory reverse re-drawing tool, the finite elements method allows to shearsh optimize dimension for this.

4.1 Characteristics of the simulation

This simulation uses the parameters in table 4 and the characteristics of DP600 and HSLA steels. The first pass is the same than previous with a drawing depth of 29,5 mm.

The second pass use a 47 mm diameter punch and has a drawing depth of 58,5 mm. Initially there is a clearance of 5,2 mm between the punch and the die on the second pass. This clearance was too high and creates undulations. (see the table of synthesis to reduce clearance). The final clearance is set at 1,2 mm but increase the stress in the sheet. Consequently we reduce the clearance on the first pass at 1,5 mm in order to reduce the stress and help the sheet move.

4.2 Increases of material abilities in a reverse redrawing process

In our case the second step's limiting draw ratio is $\beta_{2lim} = 1,33$. But the draw ratio on the second pass in the simulation ($\beta_2 = 1,75$) is over the limit. As explain in the part 2. The modification of the material history and the effect of “re-treatment” of the second pass enhanced material drawing abilities.

Tab 5 - Draw ratios of the reverse drawing FEM

	First pass	Second pass	Over All
β	1,67	1,75	2,92*
β_{lim}	1,81	1,33	

(*ratio if operation was made in a single pass).

Moreover it seems harder to evaluate the limiting draw ratio for the second pass except by realized tests or create a finite element model dedicate to this.

5. Conclusion

Once the numerical model is validate, this allow to use in combination with the laboratory trial of deep drawing in order to reduce time and cost on the drawing characterization operation.

The result of the reverse drawing simulation permit to evaluate the abilities of such a process. Secondly some important geometrical parameters (like, the clearance) were evaluate and improve the design of tools for a reverse drawing machine.

6. Acknowledgements

This work has been material and logistic funded by the National Excellence Research Project -CEEX contract no. 22/2005.

References

1. M. Banu, C. Maier, S. Bouvier, H. Haddadi, C. Teodosiu, *Data Preprocessing and Identification of the Elastoplastic Constitutive Models* - WP3, Task 1, 18-Months Progress Report, Digital Die Design Systems (3DS) IMS 199 000051, (2001), 22-29.
2. W. Johnson, P. B .Mellor, *Engineering plasticity*, ELLIS HARWOOD SERIES IN MECHANICAL ENGINEERING, 1987
3. Manuel Nemoz, *Generality on the deep drawing*, (Universite de Poitiers)
4. Amit Mukund Joshi, *Strain studies in sheet metal stamping*.

Proiectarea modelului virtual al procesului de ambutisare inversa

Rezumat

Aceasta lucrare prezinta metodologia modelarii cu elemente finite a procesului de ambutisare inversa cu scopul dezvoltarii unui model virtual al acestuia. Metoda elementelor finite permite reducerea timpului si costurilor de proiectare. De asemenea, o modelare corecta cu elemente finite permite evitarea defectelor si completarea cunostintelor privind comportarea materialului in timpul procesului de ambutisare inversa. Pentru a putea aprecia corectitudinea modelarii cu elemente finite se impune realizarea unui echipament tehnologic de laborator pentru ambutisarea inversa.

In cadrul lucrarii sunt prezentate rezultatele simularii numerice a primei etape – ambutisarea directa, rezultate care sunt validate prin cercetare experimentală. Odata validati parametrii modelului numeric, se dezvolta acesta cu scopul proiectarii si realizarii echipamentului de laborator pentru ambutisarea inversa. Al doilea obiectiv major al cercetarii prezentate in aceasta lucrare este estimarea corecta a reactiei de raspuns a materialului in timpul procesului de deformare, astfel incat sa se evite posibilele defecte de tip cute, fisuri, revenire elastica..

Conception du model virtuel du processus d'emboutissage inverse

Résumé

Ce papier présente la méthode de modélisation éléments finis du processus d'emboutissage inverse au but de développer un nouveau modèle virtuel de celui-ci. La méthode éléments finis permet de réduire le temps et le coût des activités de conception. Ensuite, une modélisation correcte aux éléments finis permet d'éviter les défauts et compléter les connaissances sur le comportement du matériau pendant le processus d'emboutissage inverse. Pour pouvoir valider la modélisation éléments finis il s'impose la fabrication d'un équipement de laboratoire pour l'emboutissage inverse.

Dans ce papier nous présentons les résultats de la simulation numérique de la première étape – l'emboutissage direct, résultats valides par la recherche expérimentale. Une fois valides les paramètres du modèle numérique, nous avons développé ce modèle au but de réaliser la conception et la fabrication de l'équipement de laboratoire pour l'emboutissage inverse. Le deuxième objectif la recherche effectuée a été la prédiction de la réaction réponse du matériau pendant le processus de mise en forme, ainsi que nous pouvons éviter les défauts possibles de type plis, fissures, retour élastique.